ACS OMEGA

http://pubs.acs.org/journal/acsodf

Article

^{68}Ga-Labeled Maleimide for Blood Pool and Lymph PET Imaging through Covalent Bonding to Serum Albumin In Vivo

Lixia Feng, Jianyang Fang, Xinying Zeng, Huanhuan Liu, Jingru Zhang, Lumei Huang, Zhide Guo,* Rongqiang Zhuang,* and Xianzhong Zhang*

Cite This: *ACS Omega* 2022, 7, 28597−28604

Read Online

ACCESS | Metrics & More | Article Recommendations | Supporting Information

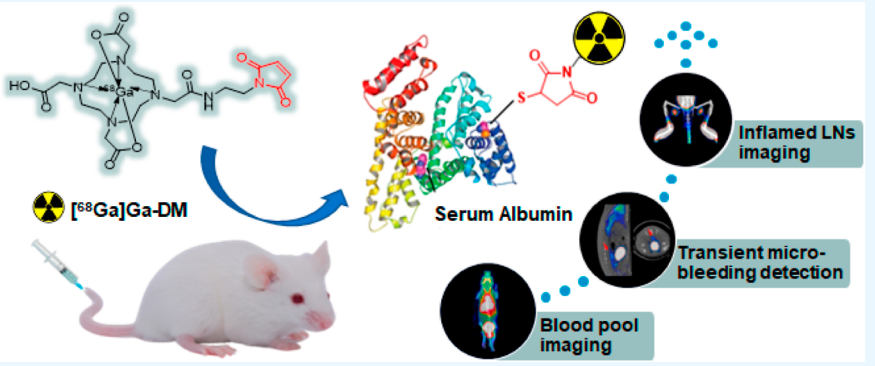

ABSTRACT: This study aims to develop a novel ^{68}Ga-labeled tracer, which can covalently bind to albumin in vivo based on the maleimide−thiol strategy, and to evaluate its potential applications using positron emission tomography (PET). ^{68}Ga-labeled maleimide-monoamide-DOTA (denoted as [^{68}Ga]Ga-DM) was prepared conveniently with a high radiochemical yield (>90%) and radiochemical purity (>99%). Its molar activity was calculated as 249.60 ± 68.50 GBq/μmol, and the octanol−water partition coefficient (Log*P*) was −3.15 ± 0.08 with good stabilities. In vitro experiments showed that [^{68}Ga]Ga-DM can bind to albumin efficiently and rapidly, with a binding fraction of over 70%. High uptake and excellent retention in blood were observed with a long half-life ($t_{1/2Z}$) of 190.15 ± 24.14 min, which makes it possible for blood pool PET imaging with high contrast. The transient micro-bleeding in the rat model was detected successfully with PET imaging. In addition, the uptakes of [^{68}Ga]Ga-DM in the inflammatory popliteal lymph nodes depend on the severity (5.90% ID/g and 2.32% ID/g vs 1.01% ID/g for healthy lymph nodes at 0.5 h post-injection) indicating its feasibility for lymphatic imaging. In conclusion, a novel ^{68}Ga-labeled tracer was prepared with high efficiency and yield in mild conditions. Based on the promising properties of bonding covalently to albumin, great stability, high blood contrast with a long half-life, and well environmental tolerance, [^{68}Ga]Ga-DM could be developed as a potential tracer for PET imaging of blood pool, bleeding, and vascular permeability alteration diseases in the clinic.

INTRODUCTION

A variety of blood pool imaging agents labeled with radionuclides have been developed, most of which are based on red blood cells (RBCs)[1−5] or plasma albumin.[6,7] Currently, ^{99m}Tc-labeled RBCs and human serum albumin ([^{99m}Tc]Tc-RBCs and [^{99m}Tc]Tc-HSA) are still used as two major agents for clinical blood pool imaging. Thinking of the low in vivo labeling efficiency,[8] RBCs need to draw blood for in vitro labeling, which is a time-consuming process with the risk of potentially infectious substances.[9] HSA is a good alternative to RBCs, but the requirement of in vitro labeling may face the problems of immunogenicity, renal elimination, and unstable biosafety activities caused by the complicated purification steps. Besides, there are problems such as poor stability,[10] high liver background uptake,[11] and low radiochemistry yield,[12] when albumin-based radiopharmaceuticals are applied to the blood pool, lymphatic detection, and other aspects. To overcome the shortcomings of in vitro labeling of albumin, radiolabeled Evans Blue (EB) dye analogues ([^{18}F]AlF-NEB, [^{64}Cu]Cu-NEB, and [^{68}Ga]Ga-NEB)[13,14] and radioiodinated 4-(*p*-iodophenyl) butyric acid ([^{131}I]IBA)[15] were developed for in vivo labeling of the endogenous albumin. However, both act by affinity adsorption of albumin, which decided that the junction is non-specific and incertitude. Furthermore, EB dye

Received: June 5, 2022
Accepted: July 15, 2022
Published: August 5, 2022

https://doi.org/10.1021/acsomega.2c03505
ACS Omega 2022, 7, 28597−28604

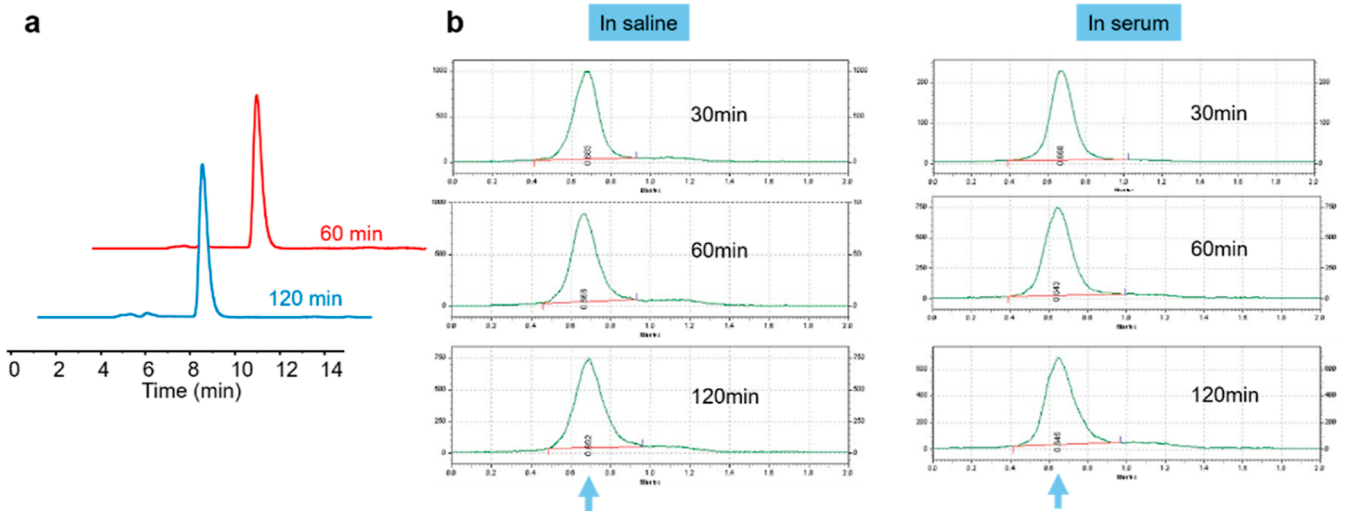

Figure 1. In vitro stabilities. (a) Radio-HPLC analysis of purified [^{68}Ga]Ga-DM after incubation in saline for 60 and 120 min, respectively. (b) Stabilities of [^{68}Ga]Ga-DM-HSA after incubation in saline and serum, respectively.

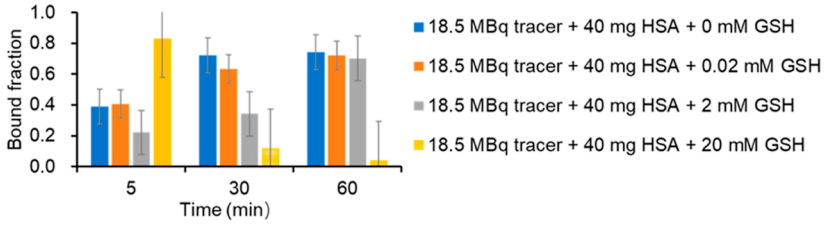

Figure 2. Bonding kinetics of [^{68}Ga]Ga-DM in vitro. The bound fraction of 18.5 MBq [^{68}Ga]Ga-DM to 40 mg/mL albumin (HSA) in the presence of 0, 0.02, 2, 20 mM GSH at 5, 30, 60 min.

has potential toxicity on fetuses. Therefore, there are still many deficiencies in existing imaging agents for clinical needs.

We noticed that there is a free thiol group in the cysteine-34 position of albumin, which accounts for about 90% of the concentration of thiol in blood plasma.[16] The cysteine-based covalent couplings are most commonly for albumin modification and are less susceptible to biological activity. Maleimides have been shown to react directly with chemical functions naturally present in biomolecules, such as thiols that are reacted by Michael's addition.[17−19] The Michael addition response between maleimide and thiol is highly selective, fast as well as mild, and it has been reported that the widespread use of maleimide−thiol coupling reactions is motivated by product stability. However, there are limited reports that maleimide−thiol adducts were tunable in a reducing environment,[20,21] resulting in instability and insecurity.[20] The capacity of reducing substances in blood and cells varies widely, with a weak reducing capacity of blood equivalent to 2−20 μM of glutathione (GSH), whereas an environment with a high reducing capacity (e.g., tumors) is equivalent to GSH of 0.5−10 mM. The albumin-binding prodrug of doxorubicin (DOXO−EMCH)[22] had been approved by the FDA, which was based on the maleimide strategy. This strategy was also reported for the prodrugs of Exatecan and SN38, released from Mal-azo-Exatecan[23] and Mal-Glu-SN38,[24] respectively.

In this paper, a novel ^{68}Ga-labeled maleimide-monoamide-DOTA (DM) is proposed, which may covalently bond to the free sulfhydryl group of serum albumin in vivo instead of reversibly binding. Thanks to the maleimide-based strategy, the complex purification steps of albumin products are avoided and damage to albumin structure and the harsh requirements for labeling conditions are reduced. Radiochemical characteristics and stability of the tracer were explored. Distribution in healthy mice and its potential for blood pool imaging, detection of bleeding, and lymphatic inflammation via positron emission tomography (PET) was assessed.

RESULTS

Radiochemistry. Preparation and analysis of ^{68}Ga-labeled tracers ([^{68}Ga]Ga-DM, [^{68}Ga]Ga-DOTA-NHS, [^{68}Ga]Ga-DM-HSA, and [^{68}Ga]Ga-DM-BSA) in this study are demonstrated in Supporting Information, Figures S1−S5. The high-performance liquid chromatography (HPLC) retention times of DM and [^{68}Ga]Ga-DM were 6.91 min and 7.31 min, respectively (Figure S1). The HPLC analysis of the mixed reaction solution after reacting for 20 min (Figure S1b) indicated a greater than 90% radiochemical yield (RCY) of [^{68}Ga]Ga-DM labeling. After purification, the radiochemical purity (RCP) of [^{68}Ga]Ga-DM was more than 99% (Figure S6). Based on the UV standard curve of the precursor (Figure S7), the molar activity (A_m) of the final tracer was calculated to be over 249.60 ± 68.50 GBq/μmol. The Log*P* of [^{68}Ga]Ga-DM was −3.15 ± 0.08 (n = 3), showing strong hydrophilicity. The in vitro stability of [^{68}Ga]Ga-DM in saline was analyzed by HPLC and the results (Figure 1a) showed that the tracer remained intact at 60 and 120 min, respectively. After being bound to albumin, the tracer maintained good stability within 2 h of incubation in saline and serum, respectively (Figure 1b).

Bonding Kinetics of [^{68}Ga]Ga-DM In Vitro. The bound fraction of [^{68}Ga]Ga-DM to albumin in vitro is shown in Figure 2. The results showed that the bound fractions of tracer to albumin at 5, 30, and 60 min were 0.39, 0.72, and 0.74,

https://doi.org/10.1021/acsomega.2c03505
ACS Omega 2022, 7, 28597−28604

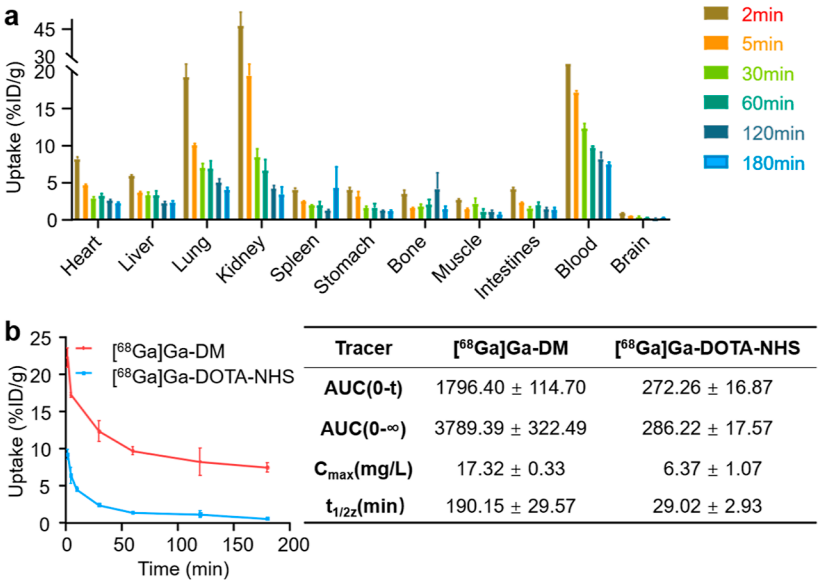

Tracer	[68Ga]Ga-DM	[68Ga]Ga-DOTA-NHS
AUC(0-t)	1796.40 ± 114.70	272.26 ± 16.87
AUC(0-∞)	3789.39 ± 322.49	286.22 ± 17.57
C_{max}(mg/L)	17.32 ± 0.33	6.37 ± 1.07
$t_{1/2z}$(min)	190.15 ± 29.57	29.02 ± 2.93

Figure 3. Biodistribution study. (a) Quantitative biodistribution analysis of [^{68}Ga]Ga-DM in healthy mice at 2, 5, 30, 60, 120, 180 min p.i.; data are expressed as mean ± SEM of injected dose per gram (%ID/g, n = 4). (b) Blood elimination curves of [^{68}Ga]Ga-DM and [^{68}Ga]Ga-DOTA-NHS (left) and the pharmacokinetic parameters (right).

respectively, indicating a highly albumin-bound ability of [^{68}Ga]Ga-DM. Then, the effect of reducing substances on the bound fraction was explored. In the presence of 0.02 mM GSH, the bound fractions were 0.40, 0.63, and 0.72, respectively (Figure 2). There was no significant difference when compared to the group without GSH addition (P = 0.0809 > 0.05), which means a reductive environment equivalent to 0.02 mM GSH did not affect the bonding of tracer to albumin. When the concentration of GSH increased to 2 mM, the tracer bound fractions decreased at 5, 30, and 60 min, which were 0.22, 0.34, and 0.70, respectively, suggesting that 2 mM GSH would affect the bonding and slow down the reaction speed, while the ratio paired t-test suggested no significant difference when compared to the group without GSH addition (P = 0.1576 > 0.05). Furthermore, when the concentration of GSH reached 20 mM, the bonding of the tracer to albumin reached 0.83 at 5 min and then showed a significant decreasing trend, reducing to 0.04 at 60 min which was significantly different from the group without GSH addition (P = 0.0288 < 0.05).

The bonding of the tracer to albumin was based on the covalent reaction of thiol and maleimide, and the reaction kinetics curve is shown in Figure S8a. Determination of the reaction order was carried out by the integral method,[25] finally, it was determined to be a second-order reaction (Figure S8b) with a binding reaction rate of about 3.69 $mol^{-1}\cdot dm^3\cdot s^{-1}$ (Figure S8c).

Biodistribution. The biodistribution results of [^{68}Ga]Ga-DM in healthy mice are shown in Figure 3a. At 2 min post-injection (p.i.), the radioactive tracer mainly accumulated in the kidneys (46.61 ± 10.71% ID/g), blood (22.22 ± 1.34% ID/g), and lungs (19.27 ± 2.62% ID/g) and less in the heart (8.12 ± 0.68% ID/g), liver (5.90 ± 0.36% ID/g), and other organs. While the kidney uptake drops rapidly to 19.46 ± 6.92% at 5 min p.i., it might be due to the unbound tracer being excreted into the urine via the kidneys. The blood uptake was observed to be highest after 5 min and hereafter p.i., the uptakes in the blood were 22.22 ± 1.34, 17.21 ± 0.34, 12.33 ± 1.37, 9.68 ± 0.56, 8.22 ± 1.84, 7.47 ± 0.65% ID/g at 2, 5, 30, 60, 120, and 180 min p.i., respectively. The pretty long circulation time of [^{68}Ga]Ga-DM indicates that the radiotracer could bound to albumin quickly and stably in vivo. Uptake ratios of blood to the other organs of interest were calculated and the high ratios guarantee the good contrast of PET images even at the early time points (Table S1).

The blood elimination curves of [^{68}Ga]Ga-DM and [^{68}Ga]Ga-DOTA-NHS were shown in Figure 3b. Compared with [^{68}Ga]Ga-DOTA-NHS, [^{68}Ga]Ga-DM showed much better blood retention, with 6.5∼13.0-fold higher blood uptakes and a 6.5-fold longer blood half-life. These results further confirmed the bonding of [^{68}Ga]Ga-DM to albumin occurred in vivo.

Blood Pool PET/CT Imaging. MicroPET/CT images of healthy mice are shown in Figure 4. The long retention of

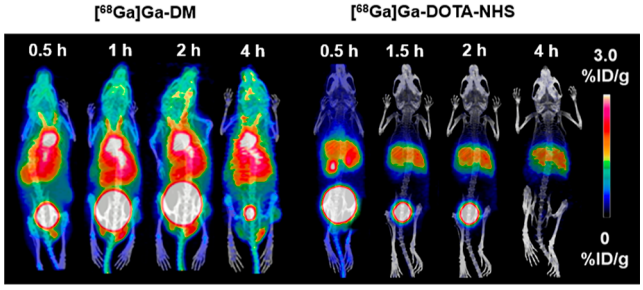

Figure 4. Maximum intensity projection PET images of [^{68}Ga]Ga-DM and [^{68}Ga]Ga-DOTA-NHS. About 11.1 MBq/100 μL of tracers were administered to each mouse intravenously. PET/CT imaging of transient micro-bleeding rat.

[^{68}Ga]Ga-DM in the blood was reconfirmed from the consistent PET images that were acquired from 0.5 h to 4 h p.i., and the radioactivity was mostly distributed in organs with sufficient vascular supply, where a "V-shaped" radioactive signal was shown at common carotid arteries. Significant accumulation of tracer in the heart contents was also observed at 0.5 h p.i. (4.32 ± 0.76% ID/g) and remain high and stable

https://doi.org/10.1021/acsomega.2c03505
ACS Omega 2022, 7, 28597−28604

uptakes at the subsequent time points. The heart content uptake at 4 h p.i. was 3.05 ± 0.49% ID/g, which reduced only 30% compared with that at 0.5 h p.i. The uptake in the heart contents was higher than that of the liver, lung, and kidney at each time point, indicating that the radiotracer might have bound to albumin and mostly concentrated in the blood, which was expected to be used for blood pool imaging in vivo. The results were consistent with those of the biodistribution experiments. The control tracer [^{68}Ga]Ga-DOTA-NHS, which may react with amino groups of other substances in the blood by activated esters was rapidly metabolized and excreted mainly into the liver and kidneys for a short period, and there was no obvious retention in the circulatory system, uptake of which was less than 0.58 ± 0.24% ID/g at 0.5 h p.i. Differences in distribution between the two could demonstrate that the maleimide structure played a key role in high blood retention of [^{68}Ga]Ga-DM.

Transient micro-bleeding SD rats were subjected to continuous 30 min dynamic PET scans to evaluate the feasibility of PET imaging with [^{68}Ga]Ga-DM for bleeding location detection. The PET images of the transient micro-bleeding model rats are shown in Figure 5. Compared with the images before colorectal wall puncture, there was a trace of radioactive in the posterior region of the bladder within 0−10 min after puncture and no significant increase at the subsequent time, with a semiquantification of 3.5-fold when compared to the uptake values before and after puncture (0.08 vs 0.28% ID/g).

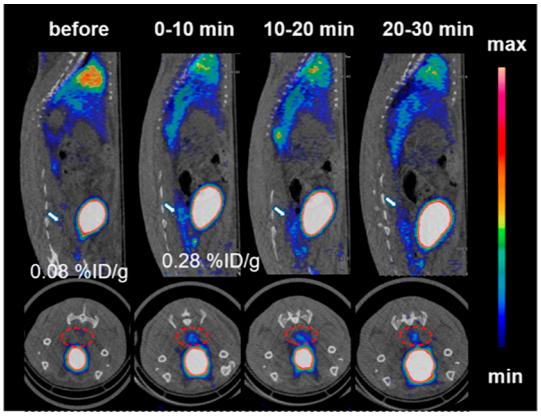

Figure 5. MicroPET/CT imaging of transient micro-bleeding rats with[^{68}Ga]Ga-DM. About 37 MBq/500 μL of [^{68}Ga]Ga-DM was injected into each rat intravenously. The white arrows (top) and red circles (bottom) represent the bleed location. PET/CT imaging of lymphadenitis model mice.

A PET/CT scan was performed to assess the feasibility of [^{68}Ga]Ga-DM for diagnosing lymph node (LN) inflammation in mice. Model mice were treated according to the procedure: (1) injection with complete Freund adjuvant into the dorsal footpad at day 0 (left: 30 μL, right: 15 μL); (2) an injection of 1.11 MBq/10 μL of [^{68}Ga]Ga-DM into the dorsal footpad and PET/CT imaging was performed after a CT scan at day 4, after a while 10 μL (1 mg/mL) of EB dye was injected to identify lymphadenitis models. As shown in Figure 6a, the CT scan showed that the LNs of the inflamed mice were significantly enlarged in contrast to healthy mice, which means a valid model was established successfully. The uptake of EB dye in the model mice reconfirmed the validation of the lymphadenitis model. PET scans were fused with CT to determine the anatomical location of the popliteal LNs, with the uptake of [^{68}Ga]Ga-DM in the left LNs of 5.90% ID/g and a 2.32% ID/g on the right, compared to the uptake of 1.01% ID/g in healthy LNs at 30 min p.i. Quantitative uptake showed increased uptake of [^{68}Ga]Ga-DM in the inflamed LNs when compared to healthy mice, which was associated with the severity of inflammation (Figure 6b). This difference was distinct at 30 min p.i, suggesting that tracers can be used for rapid diagnosis of LN inflammation.

DISCUSSION

In this study, we have successfully prepared a novel in vivo albumin-binding tracer for blood pool and lymphatic imaging, and the efficient and specific covalent binding reaction based on the maleimide and thiol group greatly improves the stability. Both [^{68}Ga]Ga-DM and [^{68}Ga]Ga-DM-HSA were stable in saline, serum, and reductive environments equivalent to 2 mM GSH. High purity tracer precursors can be commercially obtained and efficiently radio labeled with ^{68}Ga under suitable conditions. Compared with in vitro albumin radio labeling, it will not be limited by temperature, pH, and other tough conditions. The preparation of [^{68}Ga]Ga-DM is less time-consuming (15−20 min), which makes it proper for the short half-life of ^{68}Ga, and the operation is safer and more convenient compared with [^{99m}Tc]Tc-HSA, [^{99m}Tc]Tc-RBCs,[5,26] and [^{68}Ga]Ga-DOTA-HSA.[10]

Several radiolabeled molecules and peptides have been reported for versatile imaging purposes, such as [^{18}F]AlF-NEB,[13] [^{64}Cu]Cu-NEB,[13] [^{68}Ga]Ga-NEB,[14] [^{131}I]IBA,[15] and

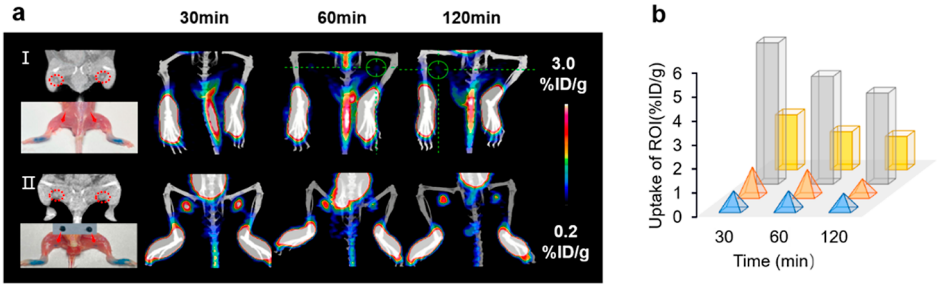

Figure 6. MicroPET/CT imaging of inflamed LNs mice with [^{68}Ga]Ga-DM. About 1.11 MBq/10 μL [^{68}Ga]Ga-DM was injected subcutaneously and then scanned at 30, 60, 120 min p.i., scale bar: 0−3% ID/g. (a) Multimodel images of LNs in different environments. CT (top left), bright light (bottom left), PET (right), circles and arrows represent popliteal LNs, and panels I and II represent healthy and inflamed LN model mice, respectively. (b) Quantitative uptakes of corresponding popliteal LNs. Left of healthy mice (blue), right of healthy mice (orange), left of inflamed LN mice (gray), right of inflamed LN mice (yellow).

https://doi.org/10.1021/acsomega.2c03505
ACS Omega 2022, 7, 28597−28604

[^{68}Ga]Ga-ABY-028.[27] They bind to serum albumins in vivo non-covalently with nanomolar (K_d = 3.4 nM for [^{68}Ga]Ga-ABY-028) to micromolar (IC_{50} = 46.5 μM for [^{131}I]IBA) binding affinities. For blood pool imaging, [^{68}Ga]Ga-DM was comparable to [^{68}Ga]Ga-NEB at 1 h p.i. and had better blood retention than [^{131}I]IBA at 3 h p.i. When compared to [^{68}Ga]Ga-ABY-028, [^{68}Ga]Ga-DM had slightly higher blood-to-liver ratio and similar blood retention within 180 min p.i. Thinking of the above tracers had been evaluated in different animal models, the head-to-head study is necessary for further detailed comparison in the future.

The binding varied significantly when the concentration of GSH was up to 20 mM. One possible cause is that there are 17 disulfide bonds in the albumin molecule, which are very sensitive to the reducing environment and prone to break to form free sulfhydryl groups.[19] When 20 mM GSH is present in the environment, strong reductive causes the disulfide bonds to be opened, and the number of free thiol groups in the reaction increases, which causes the tracer to first bond to the free thiol group of HSA, therefore, a higher bound fraction is detected at 5 min. Subsequently, the high concentration of free thiol of GSH competitive tracer resulted in a sustained decrease in the bound fraction of [^{68}Ga]Ga-DM to thiol of albumin. According to Baldwin,[20] the conclusion that free thiol groups on 10 mM reduced GSH can replace cysteine-free thiol groups in combination with maleimide under physiological conditions supports our view. In addition, the clear covalent combination mode of action has higher stability.

The strong hydrophilicity of [^{68}Ga]Ga-DM makes it reasonable that the initial uptake in the kidney is the highest and decreased quickly. We proposed that albumin unbounded tracers circulating in the blood are rapidly metabolized and excreted into the urine via the kidneys due to their strong hydrophilicity. The analysis of urine within 5 min verifies this hypothesis (Figure S9). The retention in blood at all time points was high, over 60% of activity was retained at 3 h p.i. compared with 30 min p.i. (7.47% ID/g). However, Fakhari et al.[28] reported that free ^{68}Ga can retain in the heart and blood, retaining about 1.00%ID/g at 1 h p.i. and clearing slowly. High blood retention tends to mask the problem of insufficient stability in our research. However, according to Autio et al.,[29] after an injection of ^{68}Ge/^{68}Ga generator eluate the retention of ^{68}Ga radioactivity in blood at 3 h p.i. was about 0.62% ID/g, and the PET images showed radioactive retention in the bones and joints of the limbs. In this study, much higher blood retention of [^{68}Ga]Ga-DM was observed at 3 h p.i. with negligible uptake in bones and joints of the limbs. Combined with the proven good in vitro stability, we believe that it is [^{68}Ga]Ga-DM that causes high blood retention, and it can be stable in vivo. In biodistribution studies, similar changes in retention were observed in all tissues after 30 min p.i., also indicating that the tracer was evenly distributed in vivo about 30 min after injection, with good stability. Blood-to-liver uptake ratios of [^{68}Ga]Ga-DM are higher than that of PEG ^{99m}Tc-liposomes, neutral ^{99m}Tc-liposomes, in vivo [^{99m}Tc]Tc-RBCs, in vitro [^{99m}Tc]Tc-RBCs, and [^{99m}Tc]Tc-HSA,[30] which further confirms the important value of [^{68}Ga]Ga-DM as a new PET blood pool imaging agent. Although the blood/tissue uptake values are better compared, there is still a background uptake higher than that of other organs due to the adequate blood supply of tissues such as the liver, lungs, kidneys, and spleen. High retention and proper half-life in the blood are the important features of an excellent blood pool imaging agent because there is no need to administer the drug multiple times.

According to Szucs et al.,[31] the metabolism of the maleimide structure in the tracer may form DOTA-NHS. To confirm that the tracer indeed reacts with free thiol groups in vivo through maleimide groups, a control tracer [^{68}Ga]Ga-DOTA-NHS was constructed and PET/CT imaging in mice was performed, no significant blood retention of it was observed (Figure 4). In addition, [^{68}Ga]Ga-DM-BSA was constructed in vitro and PET/CT imaging was performed to compare it with [^{68}Ga]Ga-DM. Results are shown in Figure S10, the characteristics of radioactivity retention in all organs were consistent with [^{68}Ga]Ga-DM at 0.5 h p.i., which indicates that [^{68}Ga]Ga-DM covalently binds to albumin in vivo through a maleimide structure and can be used as a PET imaging agent for pool imaging. Gel electrophoresis and autoradiography analysis of [^{68}Ga]Ga-DM cultured plasma demonstrated that 75% of the agent was bound to albumin (Figure S11 and Table S2). This was also confirmed in vitro by Zhang et al. that the maleimide structure could specifically bind to the free sulfhydryl group of cysteine at position 34 of albumin,[32] which was consistent with the study in this paper. Also, they used the characteristics of the long-time presence of fluorescent tracers in the circulatory system for the detection of sentinel LN metastasis. Although the binding of maleimide to free thiol groups in vivo is widely recognized and applied, this study still has limitations: it ignores that the radioactive signal may come from the binding of the tracer to non-albumin-free thiol. Further research is needed to fully understand the in vivo reaction in the future.

This article explored the potential application of [^{68}Ga]Ga-DM for blood pool imaging as well as bleeding point detection and lymphatic inflammation. [^{99m}Tc]Tc-sulfur colloid ([^{99m}Tc]Tc-SC) has long been used for imaging LNs as a gold standard,[33] however, it suffers from slow transport from the injection site.[34] As expected, [^{68}Ga]Ga-DM can be used to detect the lymphatic system in both physiological and pathological settings in a short time, such as inflamed LNs, in addition, the uptake of the tracer increases with the degree of inflammation.

CONCLUSIONS

A novel ^{68}Ga-labeled tracer ([^{68}Ga]Ga-DM) was developed with high efficiency and yield in mild conditions to bind to albumin in vivo covalently through a maleimide-based strategy. Our research demonstrated that tracer binding to albumin has great stability, high blood retention and contrast, and has well environmental tolerance to react. It can be applied to the detection of blood pool, bleeding, and vascular permeability alteration diseases, making it more conducive to clinical applications. The structure of [^{68}Ga]Ga-DM is simple and has a small molecular weight and may be used as a generic component to modify the targeted tracer without affecting the activity to increase absolute uptake in focus and improve pharmacokinetics.

EXPERIMENTAL SECTION

Reagents and Instruments. All materials and reagents were obtained commercially. Maleimide-monoamide-DOTA (CAS: 1006711-90-5) was purchased from MedChemExpress LLC (USA). The $^{68}GaCl_3$ solution was eluted from a ^{68}Ge/^{68}Ga generator (IREElit, Belgium). The RCY, RCP as well as A_m were detected by HPLC using a Dionex Ulti-Mate

https://doi.org/10.1021/acsomega.2c03505
ACS Omega 2022, 7, 28597−28604

3000 (Thermo Scientific, USA) with a flow-counter radioactivity detector (BioScan, USA) and by thin-layer chromatography (TLC) using a MiniScan radio scanner (BioScan, USA). The γ-counter (WIZARD 2480, PerkinElmer, USA) and CRC-25R dose calibrators (CAPIN-TEC Inc., USA) were used for the radioactivity count. PET/CT imaging was performed using an Inveon microPET/CT scanner (Siemens Medical Solutions Inc., USA).

Animal Models. Healthy BALB/c male mice (20−22 g, 6−8 weeks old), and healthy SD male rats (200−220 g, over 2 months old) were purchased from the Experimental Animal Center of Xiamen University and fed in the SPF animal room at room temperature, humidity, and plenty of food and water in a sterile environment. Animal research was carried out in accordance with the guidelines of the Animal Care and Use Committee of the Laboratory Animal Center of Xiamen University. Minimal animal deaths and injuries during the experiments.

The establishment of the transient micro-bleeding model is according to the procedure of the published literature.[35] Before the experiment, rats had fasted for 12 h, and an 18-gauge needle was inserted through the anus to puncture the rectum wall, resulting in temporary bleeding. Blood on the tip of the needle could be seen when the needle was removed.

The establishment of the lymphadenitis mouse model refers to the method of Wen et al.[15] To obtain different degrees of inflamed popliteal LNs, 15 and 30 μL of complete Freund adjuvant (Sigma Chemical) were subcutaneously injected into the bilateral toes second digits, respectively. CT imaging and EB staining were performed 4 days after injection to confirm the formation of inflammation.

Radiochemistry. The precursor maleimide-monoamide-DOTA was labeled with ^{68}Ga according to a published method with slight modifications.[36,37] Briefly, $^{68}GaCl_3$ (740 MBq) was eluted from the ^{68}Ge/^{68}Ga generator in about 1 mL of 0.1 M HCl. The solution was then mixed with a 0.05 M NH_4Ac buffer solution at pH = 5.5 to produce a final pH of 4.5, and 20 μL of 2 mg/mL precursor was added. The radiolabeling reactions were carried out by stirring at 80 °C for 15−20 min. The sample of the reaction solution was subjected to HPLC for RCY analysis with method 1 and thereafter purified with method 2 (details in the Supporting Information). Afterward, the purified solution was blow-dried with nitrogen gas and dissolved in 0.9% sodium chloride or 0.1 M PBS to give the final [^{68}Ga]Ga-DM tracer injection for the following experiments. RCP, as well as molar activity analyses for the final injection, were detected via method 1. [^{68}Ga]Ga-DOTA-NHS, [^{68}Ga]Ga-DM-has, and [^{68}Ga]Ga-DM-BSA injections were also prepared as controls, respectively (details in the Supporting Information file).

Octanol/Water Partition Coefficient. The experiment was performed according to the method used by Guo et al.[38] Briefly, about 0.1 mL of tracer solution was added to 0.9 mL phosphate-buffered solution (0.05 mol/L, pH at 7.4) in a microcentrifuge tube, then 1 mL of octanol was added and vortex-mixed for 2 min, the well-mixed solution was centrifuged at 12000 rpm for 5 min. After centrifugation, 100 μL liquid of each phase was taken for radioactivity count determination by γ-counter. The above measurement was made in triplicate. The partition coefficient value (Log*P*) was calculated and expressed as the mean ± SEM (n = 3).

Stability. The in vitro stability of the purified [^{68}Ga]Ga-DM was tested based on the previously published literature.[39] About 3.7 MBq of the tracer was incubated in 500 μL of saline for 2 h at room temperature and then monitored by HPLC via method 1 (details in the Supporting Information file) to measure the stability of the albumin-bound [^{68}Ga]Ga-DM. Purified [^{68}Ga]Ga-DM-HSA was added to 500 μL of saline and serum, respectively, kept at 37 °C up to 2 h and monitored by instant TLC (iTLC) via method 3 (details in the Supporting Information file).

Bonding Kinetics of [^{68}Ga]Ga-DM In Vitro. To explore the interaction between [^{68}Ga]Ga-DM and human serum albumin, 18.5 MBq [^{68}Ga]Ga-DM and 40 mg/mL albumin were co-incubated at 37 °C, under normal saline conditions for 5, 30, and 60 min, then the samples were treated with method 4 (details in the Supporting Information file) to obtain the bound fraction. Furthermore, the bonding fraction of [^{68}Ga]Ga-DM to albumin was also detected under GSH conditions. To explore the effect of reducing substances on the bonding of [^{68}Ga]Ga-DM to albumin, GSH was added at the incremental concentrations of 0.02, 2, and 20 mM, respectively, to mimic the in vivo blood redox environment.

To further characterize the covalent bonding kinetics of maleimide ([^{68}Ga]Ga-DM) to thiol (albumin), the radioactivity ratios of the reactants ([^{68}Ga]Ga-DM) and the products (albumin-bound [^{68}Ga]Ga-DM) were detected by iTLC via method 3 after incubation in normal saline at 37 °C for 0, 1, 2, 4, 6, 8, 10, 20, 30, and 60 min. The radioactive concentration of the reactants and products were obtained to draw the concentration−time curve and then the reaction rate was calculated accordingly.

Biodistribution Study. The biodistribution study of [^{68}Ga]Ga-DM was performed in normal Balb/c mice (18−20 g, male), which were divided into six groups by complete random grouping. About 1.11 MBq/100 μL of [^{68}Ga]Ga-DM was given intravenously via tail vein, and the mice were sacrificed at the presetting time points (2, 5, 30, 60, 120, and 180 min p.i.) by cervical dislocation. The tissues and organs of interest were separated, weighed, and detected for radioactivity by a γ-counter. The results were calculated as a percentage of the injected dose per gram of tissues (%ID/g), which were expressed as mean ± SEM (n = 4).

Blood samples at 2, 5, 30, 60, 120, and 180 min p.i. were also obtained from the biodistribution study. Uptake values and acquisition time were input to the DSA 2.0 to calculate the blood half-life of the tracer. [^{68}Ga]Ga-DOTA-NHS was used as a control.

PET/CT Imaging. Small-animal PET/CT imaging was carried out using an Inveon scanner. Mice were kept under isoflurane anesthesia with a flow rate of 0.2 mL/min and heated to 37 °C in the prone position. The images were reconstructed with OSEM3D/OP−MAP algorithm by the software Inveon Research Workplace.

For healthy mice imaging, 11.1 MBq/100 μL of [^{68}Ga]Ga-DM was administered intravenously via mouse tail vein, and scans were performed at 0.5, 1, 2, and 4 h p.i. PET imaging of healthy mice with [^{68}Ga]Ga-DOTA-NHS and [^{68}Ga]Ga-DM-BSA was also conducted, respectively, for comparison.

For the transient micro-bleeding imaging, about 37 MBq/500 μL of [^{68}Ga]Ga-DM was administered intravenously via rat tail vein, and subsequently, a 30 min dynamic PET imaging was performed immediately after tracer injection to detect bleeding.

For the imaging of lymphadenitis model mice, about 1.11 MBq/10 μL of [^{68}Ga]Ga-DM was subcutaneously adminis-

https://doi.org/10.1021/acsomega.2c03505
ACS Omega 2022, 7, 28597−28604

tered to the second digit of bilateral toes 30 min before the scan, then scans were performed at 0.5, 1, and 2 h, respectively. PET imaging of healthy LNs of control mice was performed for comparison.

Statistical Analysis. Statistical analyses were performed using the software GraphPad Prism 9.0 (Insightful Science LLC, USA). Differences between groups were compared by the ratio paired *t*-test, and the significance level was set to 0.05.

■ ASSOCIATED CONTENT

Supporting Information

The Supporting Information is available free of charge at https://pubs.acs.org/doi/10.1021/acsomega.2c03505.

Methods of HPLC and iTLC; ultrafiltration method; covalent binding reaction rate calculation; supplemental HPLC profiles; PET/CT images of [^{68}Ga]Ga-DM-BSA; and gel electrophoresis and autoradiography analysis of [^{68}Ga]Ga-DM cultured plasma (PDF)

■ AUTHOR INFORMATION

Corresponding Authors

Zhide Guo − *State Key Laboratory of Molecular Vaccinology and Molecular Diagnostics & Center for Molecular Imaging and Translational Medicine, School of Public Health, Xiamen University, Xiamen 361102, China*; Email: gzd666888@xmu.edu.cn

Rongqiang Zhuang − *State Key Laboratory of Molecular Vaccinology and Molecular Diagnostics & Center for Molecular Imaging and Translational Medicine, School of Public Health, Xiamen University, Xiamen 361102, China*; Email: zhrq@xmu.edu.cn

Xianzhong Zhang − *State Key Laboratory of Molecular Vaccinology and Molecular Diagnostics & Center for Molecular Imaging and Translational Medicine, School of Public Health, Xiamen University, Xiamen 361102, China*; orcid.org/0000-0001-8591-8301; Email: zhangxzh@xmu.edu.cn

Authors

Lixia Feng − *State Key Laboratory of Molecular Vaccinology and Molecular Diagnostics & Center for Molecular Imaging and Translational Medicine, School of Public Health, Xiamen University, Xiamen 361102, China*

Jianyang Fang − *State Key Laboratory of Molecular Vaccinology and Molecular Diagnostics & Center for Molecular Imaging and Translational Medicine, School of Public Health, Xiamen University, Xiamen 361102, China*

Xinying Zeng − *State Key Laboratory of Molecular Vaccinology and Molecular Diagnostics & Center for Molecular Imaging and Translational Medicine, School of Public Health, Xiamen University, Xiamen 361102, China*

Huanhuan Liu − *State Key Laboratory of Molecular Vaccinology and Molecular Diagnostics & Center for Molecular Imaging and Translational Medicine, School of Public Health, Xiamen University, Xiamen 361102, China*

Jingru Zhang − *State Key Laboratory of Molecular Vaccinology and Molecular Diagnostics & Center for Molecular Imaging and Translational Medicine, School of Public Health, Xiamen University, Xiamen 361102, China*

Lumei Huang − *State Key Laboratory of Molecular Vaccinology and Molecular Diagnostics & Center for Molecular Imaging and Translational Medicine, School of Public Health, Xiamen University, Xiamen 361102, China*

Complete contact information is available at: https://pubs.acs.org/10.1021/acsomega.2c03505

Author Contributions

L.F., J.F., and R.Z. designed the preparation of the radiolabeled compounds. L.F., X.Z., and H.L. performed the in vitro characterization of the compounds. L.F., Z.G., R.Z., and X.Z. designed the in vitro and in vivo assays. L.F., J.F., J.Z., and L.H. performed and analyzed the assays and created the images. L.F., X.Z., R.Z., and Z.G. contributed to the writing of the manuscript. All authors have approved the final version of the manuscript.

Notes

The authors declare no competing financial interest.

■ ACKNOWLEDGMENTS

This study was financially supported by the National Natural Science Foundation of China (21906135, 81901805, 21976150), Major Research Plan of the National Natural Science Foundation of China (91959122), and Joint Fund of the National Natural Science Foundation of China—China National Nuclear Corporation for Nuclear Technology Innovation (U1967222).

■ LIST OF ABBREVIATIONS

PET, positron emission tomography
CT, computed tomography
DM, maleimide-monoamide-DOTA
RCY, radiochemical yield
RCP, radiochemical purity
A_m, molar activity
Log*P*, octanol−water partition coefficient
LNs, lymph nodes
EB, Evans Blue
p.i., post-injection
RBCs, red blood cells
BSA, bovine serum albumin
HSA, human serum albumin
HPLC, high-performance liquid chromatography
iTLC, instant thin-layer chromatography
GSH, glutathione

■ REFERENCES

(1) Burroni, B.; Borsari, B.; Pichierri, P.; Polito, P.; Toscano, T.; Grassetto, G.; Al-Nahhas, A.-N.; Rubello, R.; Vattimo, V. Preoperative diagnosis of orbital cavernous hemangioma: a ^{99m}Tc-RBC SPECT study. *Clin. Nucl. Med.* **2012**, *37*, 1041−1046.

(2) Haghighatafshar, H.; Gheisari, G.; Ghaedian, G. Importance of heparin provocation and SPECT/CT in detecting obscure gastrointestinal bleeding on ^{99m}Tc-RBC scintigraphy. *Medicine* **2015**, *94*, No. e1325.

(3) Provost, K.; Charest, M. Detection of intrathoracic bleeding by ^{99m}Tc-labeled red blood cell SPECT/CT after wedge biopsy of pulmonary angiosarcoma. *J. Nucl. Med. Technol.* **2016**, *44*, 205−206.

(4) Liu, M.; Zhao, Z.; Fang, W.; Liu, S. Novel approach for ^{99m}Tc-Labeling of red blood cells: evaluation of ^{99m}Tc-4SAboroxime as a blood pool imaging agent. *Bioconjugate Chem.* **2017**, *28*, 2998−3006.

(5) Kang, S.; Moon, B.; Kim, H.; Yoon, H.; Kim, B. ^{99m}Tc-RBC SPECT/CT for duodenal bleeding point detection. *Clin. Nucl. Med.* **2020**, *45*, e411−e412.

(6) Lambert, B.; Mertens, J.; Sturm, E.; Stienaers, S.; Defreyne, L.; D'Asseler, Y. ^{99m}Tc-labelled macroaggregated albumin (MAA)

scintigraphy for planning treatment with ^{90}Y microspheres. *Eur. J. Nucl. Med. Mol. Imag.* **2010**, *37*, 2328−2333.
(7) De la Garza-Ramos, C.; Muneer, M.; Lewis, J.; Harnois, D.; Taner, C.; Frey, G.; Rosser, B.; Toskich, B. Transportal technetium-99m-labeled macroaggregated albumin scintigraphy to quantify occult intrahepatic microvascular portosystemic shunting. *J. Radiol. Case Rep.* **2021**, *16*, 975−978.
(8) Patrick, S.; Glowniak, J.; Turner, F.; Robbins, M.; Wolfangel, R. Comparison of in vitro RBC labeling with the UltraTag RBC Kit Versus in vivo labeling. *J. Nucl. Med.* **1991**, *32*, 242.
(9) Lodhi, N.; Park, J.; Kim, K.; Kim, Y.; Shin, J.; Lee, Y.; Im, H.; Jeong, J.; Khalid, M.; Cheon, G.; Lee, D.; Kang, K. Development of ^{99m}Tc-labeled human serum albumin with prolonged circulation by chelate-then-click approach: a potential blood pool imaging agentr. *Mol. Pharm.* **2019**, *16*, 1586−1595.
(10) Jain, A.; Pandey, U.; Gamre, N.; Sarma, H.; Dash, A. Development of ^{68}Ga labeled human serum albumin for blood pool imaging: a comparison between two ligands. *J. Radioanal. Nucl. Chem.* **2017**, *313*, 661−668.
(11) Gholipour, G.; Akhlaghi, A.; Kheirabadi, K. M.; Ramandi, R. F.; Farashahi, F.; Beiki, B.; Jalilian, R. Development of a novel ^{68}Ga-dextran carboxylate derivative for blood pool imaging. *Radiochim. Acta* **2019**, *107*, 233−242.
(12) Basuli, F.; Li, C.; Xu, B.; Williams, M.; Wong, K.; Coble, V.; Vasalatiy, O.; Seidel, J.; Green, M.; Griffiths, G.; Choyke, P.; Jagoda, E. Synthesis of fluorine-18 radio-labeled serum albumins for PET blood pool imaging. *Nucl. Med. Biol.* **2015**, *42*, 219−225.
(13) Niu, G.; Lang, L.; Kiesewetter, D.; Ma, Y.; Sun, Z.; Guo, N.; Guo, J.; Wu, C.; Chen, X. In vivo labeling of serum albumin for PET. *J. Nucl. Med.* **2014**, *55*, 1150−1156.
(14) Zhang, J.; Lang, L.; Zhu, Z.; Li, F.; Niu, G.; Chen, X. Clinical Translation of an Albumin-Binding PET Radiotracer ^{68}Ga-NEB. *J. Nucl. Med.* **2015**, *56*, 1609−1614.
(15) Wen, X.; Shi, C.; Xu, D.; Zhang, P.; Li, Z.; Li, J.; Su, X.; Zhuang, R.; Liu, T.; Guo, Z.; Zhang, X. Radioiodinated portable albumin binder as a versatile agent for in vivo imaging with single-photon emission computed tomography. *Mol. Pharm.* **2019**, *16*, 816−824.
(16) Jacobson, O.; Kiesewetter, D.; Chen, X. Albumin-binding evans blue derivatives for diagnostic imaging and production of long-acting therapeutics. *Bioconjugate Chem.* **2016**, *27*, 2239−2247.
(17) Renault, K.; Fredy, J.; Renard, P.; Sabot, C. Covalent modification of biomolecules through maleimide-based labeling strategies. *Bioconjugate Chem.* **2018**, *29*, 2497−2513.
(18) Fontaine, S.; Reid, R.; Robinson, L.; Ashley, G.; Santi, D. Long-term stabilization of maleimide-thiol conjugates. *Bioconjugate Chem.* **2015**, *26*, 145−152.
(19) St. Amant, A.; Lemen, D.; Florinas, S.; Mao, S.; Fazenbaker, C.; Zhong, H.; Wu, H.; Gao, C.; Christie, R.; de Alaniz, J. R. Tuning the Diels-Alder Reaction for Bioconjugation to Maleimide Drug-Linkers. *Bioconjugate Chem.* **2018**, *29*, 2406−2414.
(20) Baldwin, A.; Kiick, K. Tunable degradation of maleimide-thiol adducts in reducing environments. *Bioconjugate Chem.* **2011**, *22*, 1946−1953.
(21) Lin, D.; Saleh, S.; Liebler, D. Reversibility of covalent electrophile-protein adducts and chemical toxicity. *Chem. Res. Toxicol.* **2008**, *21*, 2361−2369.
(22) Kratz, F. DOXO-EMCH (INNO-206): the first albumin-binding prodrug of doxorubicin to enter clinical trials. *Expert Opin. Invest. Drugs* **2007**, *16*, 855−866.
(23) Cheng, Z.; Huang, Y.; Shao, P.; Wang, L.; Zhu, S.; Yu, J.; Lu, W. Hypoxia-activated albumin-binding exatecan prodrug for cancer therapy. *ACS Omega* **2022**, *7*, 1082−1089.
(24) Huang, Y.; Wang, L.; Cheng, Z.; Yang, B.; Yu, J.; Chen, Y.; Lu, W. SN38-based albumin-binding prodrug for efficient targeted cancer chemotherapy. *J. Controlled Release* **2021**, *339*, 297−306.
(25) Bagshaw, C. Order of reaction. In *Encyclopedia of Biophysics*; Roberts, G., Ed.; Academic Press: Springer Berlin Heidelberg, 2013; pp 1807−1808.
(26) Nishimura, T.; Hamada, S.; Hayashida, K.; Uehara, T.; Katabuchi, T.; Hayashi, M. Cardiac blood-pool scintigraphy using technetium-99m DTPA-HSA: comparison with in vivo technetium-99m RBC labeling. *J. Nucl. Med.* **1989**, *30*, 1713−7.
(27) Jussing, E.; Lu, L.; Grafström, J.; et al. [^{68}Ga]ABY-028: an albumin-binding domain (ABD) protein-based imaging tracer for positron emission tomography (PET) studies of altered vascular permeability and predictions of albumin-drug conjugate transport. *EJNMMI Res.* **2020**, *10*, 106.
(28) Fakhari, A.; Jalilian, A.; Johari-Daha, F.; Shafiee-Ardestani, M.; Khalaj, A. Preparation and biological study of ^{68}Ga-DOTA-alendronate. *Asia Ocean. J. Nucl. Med. Biol.* **2016**, *4*, 98−105.
(29) Autio, A.; Virtanen, H.; Tolvanen, T.; Liljenbäck, H.; Oikonen, V.; Saanijoki, T.; Siitonen, R.; Käkelä, M.; Schüssele, A.; Teräs, M.; Roivainen, A. Absorption, distribution and excretion of intravenously injected ^{68}Ge/^{68}Ga generator eluate in healthy rats, and estimation of human radiation dosimetry. *EJNMMI Res.* **2015**, *5*, 40.
(30) Beth, G.; William, T.; Robert, K. Blood-pool imaging using technetium-99m labeled liposomes. *J. Nucl. Med.* **1996**, *37*, 1374−1379.
(31) Driver, Z.; Ebenhan, I.; Szucs, R.; Parker, J. R.; Zeevaart, T.; Hunter, C. Towards the development of a targeted albumin-binding radioligand for theranostic applications: synthesis, radiolabelling and preliminary in vivo studies. *Nucl. Med. Biol.* **2021**, *94*−*95*, 53−66.
(32) Zhang, W.; Song, S.; Wang, H.; Wang, Q.; Li, D.; Zheng, S.; Xu, Z.; Zhang, H.; Wang, J.; Sun, J. In vivo irreversible albumin-binding near-infrared dye conjugate as a naked-eye and fluorescence dual-mode imaging agent for lymph node tumor metastasis diagnosis. *Biomaterials* **2019**, *217*, 119279.
(33) Hung, J.; Wiseman, G.; Wahner, H.; Mullan, B.; Taggart, T.; Dunn, W. Filtered technetium-99m-sulfur colloid evaluated for lymphoscintigraphy. *J. Nucl. Med.* **1995**, *36*, 1895−901.
(34) Wang, Y.; Lang, L.; Huang, P.; Wang, Z.; Jacobson, O.; Kiesewetter, D.; Ali, I.; Teng, G.; Niu, G.; Chen, X. In vivo albumin labeling and lymphatic imaging. *Proc. Natl. Acad. Sci. U.S.A.* **2015**, *112*, 208−213.
(35) Zhang, X.; Wang, L.; Fu, W.; Feng, Y.; Zeng, C.; Zhou, L.; Zhang, T.; Xu, T.; Cao, J.; Li, Z.; Chen, Y. ^{18}F-PEG$_1$-vinyl sulfone-labeled red blood cells as positron emission tomography agent to image intra-abdominal bleeding. *Front. Med.* **2021**, *8*, 646862.
(36) Beaino, W.; Nedrow, J.; Anderson, C. Evaluation of ^{68}Ga- and ^{177}Lu-DOTA-PEG4-LLP2A for VLA-4-Targeted PET imaging and treatment of metastatic melanoma. *Mol. Pharm.* **2015**, *12*, 1929−1938.
(37) Ujula, T.; Salomäki, S.; Virsu, P.; Lankinen, P.; Mäkinen, T.; Autio, A.; Yegutkin, G.; Knuuti, J.; Jalkanen, S.; Roivainen, A. Synthesis, ^{68}Ga labeling and preliminary evaluation of DOTA peptide binding vascular adhesion protein-1: a potential PET imaging agent for diagnosing osteomyelitis. *Nucl. Med. Biol.* **2009**, *36*, 631−641.
(38) Guo, Z.; Zhang, P.; Song, M.; Wu, X.; Liu, C.; Zhao, Z.; Lu, J.; Zhang, X. Synthesis and preliminary evaluation of novel ^{99m}Tc-labeled folate derivative via click reaction for SPECT imaging. *Appl. Radiat. Isot.* **2014**, *91*, 24−30.
(39) Mou, T.; Jing, H.; Yang, W.; Fang, W.; Peng, C.; Guo, F.; Zhang, X.; Pang, Y.; Ma, Y. Preparation and biodistribution of [^{18}F]FP2OP as myocardial perfusion imaging agent for positron emission tomography. *Bioorg. Med. Chem.* **2010**, *18*, 1312−1320.

https://doi.org/10.1021/acsomega.2c03505
ACS Omega 2022, 7, 28597−28604